

# Depinning transition for a screw dislocation in a model solid solution

S. Patinet and L. Proville

*CEA, DEN, Service de Recherches de Métallurgie Physique, F-91191 Gif-sur-Yvette, France*

(Dated: November 9, 2020)

On the basis of the classical dislocation theory, the solid solution hardening (SSH) is commonly ascribed to the pinning of the edge dislocations. At the atomic level, the theoretical study of the dislocation cores contrasts with such a prediction. Using the static molecular simulations with some interatomic effective potentials, we demonstrate numerically that the critical resolved shear stress associated with a screw dislocation in a random Ni(Al) single crystal has same order as the edge one. Such a result is imposed by the details of the dislocation stacking fault and the core dissociation into Shockley partials. The SSH statistical theory is employed to tentatively predict analytically the data acquired through our atomistic simulations at different Al concentration.

PACS numbers: 62.20.F-, 83.60.La

## I. INTRODUCTION

In the alloy manufacturing the solid solution hardening (SSH) is a standard process which allows to increase the yield stress of a material by dispersion of some atomic-sized obstacles across the dislocation glide. The choice of the impurity and which proportion is required is an important issue in the commercial alloy design.<sup>1,2</sup> On the condition that these impurities remain in solution, favored either by a thermal treatment or the alloy thermodynamics, the microstructure is unchanged but the dislocations are pinned by the randomly distributed obstacles. The dislocation pinning yields an increase in the material strength without involving large inhomogeneities such as inclusions or grain boundaries, by contrast to the other methods as the precipitation strengthening or the strain hardening.

The dislocation impinging on a random distribution of obstacles is a standard problem of the theoretical metallurgy<sup>3,4,5,6,7,8,9,10</sup> and the statistical physics<sup>11,12,13,14,15</sup> as well. Only recently this problem could have been addressed with some three-dimensional atomistic simulations<sup>16,17,18,19,20,21,22,23,24,25</sup> that shed a new light on points that were still a matter of debate in material science. However the difficulty of developing reliable inter-atomic potentials for modeling dislocations in alloys confines the atomistic simulations to only few systems. The Ni(Al)  $\gamma$ -phase is one of them and corresponds to the prototypical case for the binary substitutional alloys with a high order energy and a high solubility limit, about  $C_{Al} = 10$  at. % which involves a broad concentration range for the stability of the solid solution.

The static atomistic simulations allow to compute the Critical Resolved Shear Stress (CRSS) for an isolated dislocation in a single crystal of a purely random solution.<sup>18,24,25</sup> In the model Ni(Al) solution, the CRSS associated with an edge dislocation was found<sup>25</sup> to increase roughly linearly at a rate of about 30 MPa per atomic percent. This result agrees with the experimental data on the Ni(Al) hardness<sup>1</sup> ( $H$ ) from which the flow stress  $\sigma$  can be deduced by application of the empirical linear relation<sup>26,27</sup>  $H = 3\sigma$  (valid for metallic crystalline

materials). The main question raised by such a result bears on the role of the screw dislocation segments. According to a widespread belief drawn on the first order elastic dislocation theory (see text book as Ref. 28), the screw dislocation CRSS would be smaller than the edge one. By contrast, our present atomistic study shows that the screw CRSS has same order as the edge one for different Al densities  $C_{Al}$ , between 2 at. % and 12 at. %. We analyze our results in terms of the interaction between the dislocation core and some isolated obstacles either single Al placed at different positions around the glide plane or Al dimers with different positions, orientations and bond lengths. The dominant component of the dislocation pinning is found to be a short range interaction of typically few Burgers vector between the obstacles and the distinct Shockley partials of the dissociated dislocation. This rather short range interaction is to be compared with the partial cores which spread over few lattice spacings.<sup>29,30</sup> Our systematic study of every dimer configuration allows us to enhance the role of the chemical interaction between nearest solutes which yields some pinning strengths that diverge from the simple superposition of the strain fields due to each solute.

In addition to provide some data about the strength of a single Ni(Al) crystal, our atomistic simulations allow us to challenge the different versions of the statistical theory for the SSH.<sup>3,4,5,6,7,8,9</sup> The corresponding analytical models intend to provide an estimate of the CRSS from the elementary interaction between a single dislocation and an isolated obstacle. Most of the other effects on the dislocation pinning as the presence of the grain boundaries, the dislocation forest and the thermal activation of the solute motion are assumed not to play an important role. This proves to match the conditions of our numerical simulations which permits us to compare the theoretical predictions to the simulation data. A common point to the different versions of the SSH theory is to have been derived in the framework of the continuous line tension model where the dislocation is thought of as an elastic string anchored by a single type of obstacles. The split between the different versions of the theory stems from the various assumptions made on the critical string con-

figuration and how the depinning proceeds. For the sake of consistency, the string-obstacle interaction parameters are determined from our atomistic study and the statistical models end results are compared to our direct computation of the CRSS for the Ni(Al) single crystal. Among the theories proposed to compute the CRSS, we show that some of them quantitatively agree with our computations for the concentrated solid solutions, i.e.  $2 \text{ at. } \% < C_{Al} < 12 \text{ at. } \%$ . The concordance of the atomistic simulations and the SSH continuous theory confirms the plausibility of a multi-scale approach to the plastic flow in the inhomogeneous media.

The present paper is organized as follows: In Sec. II, the atomistic method to compute the CRSS for a screw dislocation is described and the results are compared to the edge ones. In Sec. III, the different analytical models for SSH are presented and discussed in regard of our atomistic simulations. In Sec. IV, our study is resumed and our future works announced.

## II. MOLECULAR STATIC COMPUTATION OF THE SOLUTION STRENGTH

By contrast to the phenomenological line tension approach applied to the SSH,<sup>31,32</sup> the atomistic simulation allows to capture the main physical aspect of the dislocation core by integrating the nonlinear many-body interactions between the atoms displaced during the dislocation course. In our simulations the atomic interactions are modeled through the embedded atom method (EAM) the detail of which has been published elsewhere.<sup>19,33,34</sup> One must notice that two typo errors must be corrected before implementing the EAM potentials. For the Ni-Ni interaction see Ref. 35 and for the Ni-Al interaction the coefficients  $g_{Ni}$  and  $g_{Al}$  must be exchanged in Ref. 19. According to private communications with other authors these corrections have been taken into account in other earlier works using the same method. The simulation cell (see Fig.1) is oriented so as that the horizontal Z planes are the  $(1\bar{1}1)$  of the face centered cubic (fcc) lattice while the Y direction corresponds to the screw Burgers vector  $b = [110]a_0/2$  and the X direction is orthogonal to Z and Y and points at the dislocation motion. The simulation box size along the directions  $i = X, Y, Z$  is denoted by  $L_i$ . The periodic boundary conditions are applied along X and Y while the external applied stress  $\tau_{yz}$  is produced by imposing extra forces to the atoms in the upper and lower Z surfaces.<sup>16</sup> In order to form a screw dislocation between the two  $(1\bar{1}1)$  central mid-planes, the displacement field of the elastic solution for a dissociated screw with Burgers vector  $b$  is applied to the atoms of the simulation box. In order to compensate the Burgers vector shift at the crossing of the boundaries along X, the corresponding periodic boundary conditions are tilted from  $b$  alongside Y. The ideal solid solution is then formed by substituting randomly Ni atoms with Al in the proportion fixed by the Al atomic density  $C_{Al}$ .

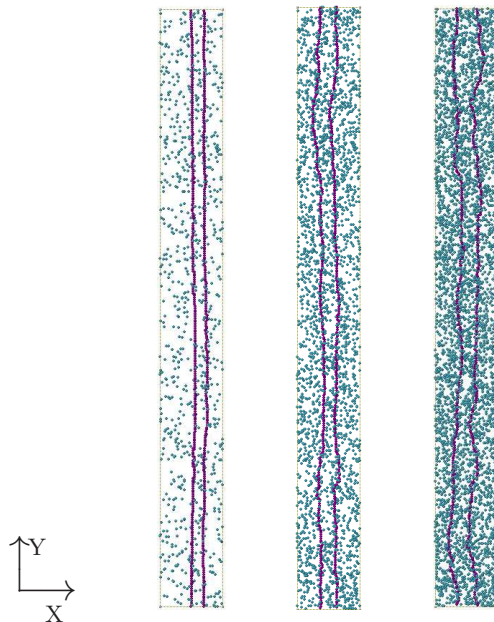


FIG. 1: (color online) View of the  $(1\bar{1}1)$  glide plane and the dissociated screw dislocation in the Ni(Al) simulated solution at various concentrations:  $C_{Al} = 2 \text{ at. } \%$  (lhs),  $C_{Al} = 6 \text{ at. } \%$  (center) and  $C_{Al} = 10 \text{ at. } \%$  (rhs). The box size is 300 b along Y, 32 b along X and 34 b along Z (orthogonal to this paper sheet). The Shockley partials are colored in violet and the Al atoms in blue. The external shear stress has been fixed to one half of the CRSS.

The solute distribution depends on the *seed* of the numerical random generator. For each  $C_{Al}$  ranging from 2 to 12 at. %, several distributions have been generated. The Molecular Statics (MS) simulations are performed to minimize the total enthalpy under a fixed applied shear stress. The external applied stress is incremented by 0.3 MPa and for each increment the minimization procedure is repeated until it either converges to a required precision or the dislocation starts to glide. To minimize the size effects in the simulations of the random solution, we chose  $L_y = 300b$  which allows to neglect the interaction between an obstacle and its periodic image and to achieve satisfactory statistics. The same method with same inter-atomic potentials have been employed in Ref. 25 for the edge dislocation.

In Fig.1 we reported a snapshot of three typical systems computed for an external shear stress smaller than the CRSS  $\tau_c$ . The atoms involved into the partials are recognized by their default configurations in first neighbor positions. The Al atoms that participate to the  $(1\bar{1}1)$  planes that bound the glide plane have also been reported on these 3 pictures. The screw dislocation oscillates in the crystal in a way similar to the edge one as reported earlier.<sup>25</sup> It is worth noticing that such a wavy profile has been observed experimentally<sup>36</sup> in some other type of solid solution as Cu(Al) and Cu(Si). The dislocation does not form large bow between well separated pinning

points but rather conserves a wavy shape. Such configurations of the dislocation impinging on a random solution do not correspond to the one obtained within a phenomenological elastic string model as the one used for instance in the work of Foreman and Makin.<sup>31</sup> The reason is threefold: (i) the solution is concentrated and thus the isolated point like obstacles are rare, (ii) the interaction dislocation-obstacle is not a point-like force and (iii) the pinning strength of the Al obstacle is much weaker than what can be estimated through the elastic stress-strain field of a Volterra dislocation. As detailed further (see Tab.I, the pinning strength of an isolated Al on the screw dislocation is about one hundredth of the line tension meanwhile the elastic theory in a very first order version would predict one order larger.

In our MS simulations when the dislocation moves freely, we let it glide for ten passages in the simulation box in order to probe possible stronger pinning configurations created by the relative displacement of one Burgers vector  $b$  at each passage between the plane above and below the glide plane. Since  $L_x \approx 32 b$ , we assume that when the dislocation has glided over  $10 \times L_x$  we reach the maximum of the applied shear stress for the considered random distribution. Such a glide distance has the same order as the mean free path of a gliding dislocation through the forest dislocations in a metallic polycrystal where the dislocation density may reach  $10^9 \text{ cm}^{-2}$ . In most of our computations the dislocation does not encounter a new pinning configuration after 4 passages in the simulation box. For each concentration, the calculations of the CRSS,  $\tau_c$  from various distributions have been reported in Fig.2 (a) where each open symbol corresponds to a different random distribution. The dispersion on the measure of  $\tau_c$  is related to the finite size effect along Y. The choice of the suitable  $L_y$  results from a compromise between the computational load and the statistics.

The order of magnitude of the solution strengthening is about 30 MPa per atomic percent of Al which is noteworthy similar to the edge one, obtained from Ref. 25 and reported in Fig.2 (b) for further comparison with the analytical models. Such a result contrasts seriously with the classical calculations based on the elastic theory of dislocation.<sup>32</sup> However this can be fairly understood from the analysis of the interaction between the dislocation and a single obstacle at the atomistic level. We carried out the same type of MS simulations as for the random solid solution except that only one isolated Al atom is placed in a simulation cell of pure Ni. Then the external shear stress  $\tau_{yz}$  is incremented from zero to  $\tau_m$  at which the dislocation liberates. Since the simulation cell is periodic along Y, the obstacle and its periodic images form a regular array of obstacles separated by  $L_y$ . The balance between the Peach-Koehler force and the obstacle pinning leads to  $f_m = (\tau_m - \tau_p)bL_y$  where  $\tau_p$  is the screw Peierls stress and  $b$  is the Burger vector of the whole dislocation. Because of the nonlinearity of the atomic interactions, we found that the pinning strength of an

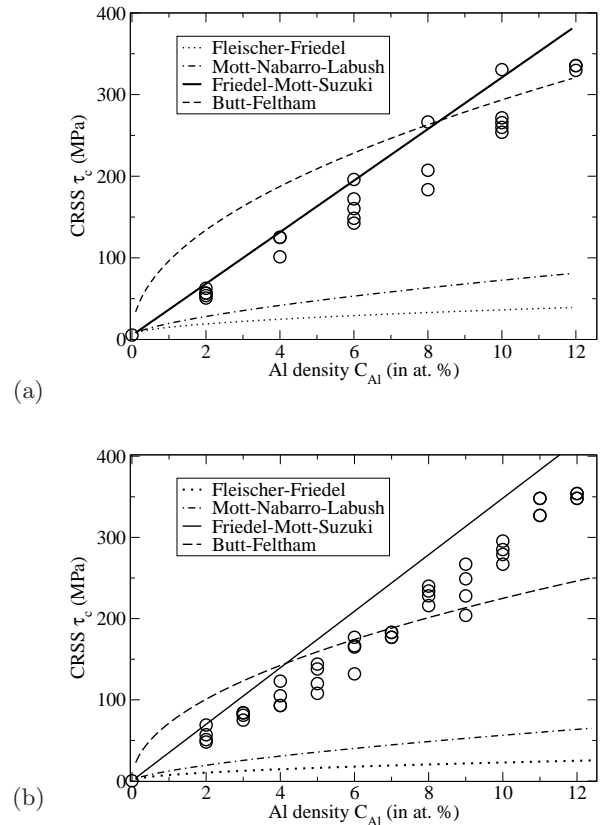


FIG. 2: Variation of the critical resolved shear stress  $\tau_c$  for a screw dislocation (a) and for an edge dislocation (b) against the Al concentration  $C_{Al}$  computed from the MS simulations with different Al random distributions (symbols). The estimations made with the analytical models have also been reported: Fleischer-Friedel<sup>37</sup> (dotted line), Friedel-Mott-Suzuki<sup>6</sup> (full line), Mott-Nabarro-Labusch<sup>5</sup> (dot-dashed line) and Butt-Feltham<sup>9</sup> (dashed line).

isolated obstacle depends on its place above or below the glide plane as well as on which partial is concerned. Our results are reported on the first lines of Tab.I where the corresponding strength  $f_m$  has been normalized by the constant  $\mu b^2$  to provide the standard pinning coefficient denoted by  $\alpha$ . We choose  $\mu = 74600 \text{ MPa}$ , the shear modulus for the Ni (111) planes  $[c_{11} - c_{12} + c_{44}]/3$ . Although the normalization has been realized with the value of  $\mu b^2$  for pure Ni, one must bear in mind that this normalization is a conventional way to present the result. In Tab.I the single obstacle denoted by (a1) corresponds to an isolated Al placed in the  $(\bar{1}\bar{1}1)$  plane situated just above the glide plane while (b1) is for an Al which participates in the  $(\bar{1}\bar{1}1)$  plane just below the glide plane. The pinning strength of a single Al atom is found to have the same magnitude as for the edge dislocation<sup>25</sup> which confirms our results about the same solid solution CRSS for both edge and screw dislocations. The strengths of some isolated Al have also been reported in Tab.I, for the farther  $(\bar{1}\bar{1}1)$  planes. For the second nearest one, the pinning

forces are referenced by (a2) and (b2) for the Al above and below the glide plane, respectively. For the third nearest planes, the pinning forces are arranged in same order and referenced by (a3) and (b3).

On the condition that the dislocation core distance to the obstacle remains larger than the core extent, it is possible to analyze the interaction in terms of the continuous elastic theory. We intend applying such an approach for the obstacles situated in the third ( $1\bar{1}1$ ) plane from the glide plane. For that case, the potential landscape of the dissociated screw dislocation (dot-dashed line in Fig. 3) has the form  $\beta z[1/(z^2 + (x+d)^2) - 1/(z^2 + x^2)]$ , i.e. the one for two opposite edge dislocations separated from  $d$ , the dissociation distance.<sup>6,8,28</sup> According to the elastic theory, the interaction pre-factor  $\beta$  is given by  $\frac{\mu b^*}{3\pi} \frac{1+\nu}{1-\nu} (\Delta V)$  where  $\nu$  is the Ni Poisson coefficient,  $\Delta V$  is the atomic volume variation due to the Al impurity in Ni. If one neglects the interaction between the obstacle and the farthest partial, the corresponding pinning coefficient for a single partial is thus  $\alpha = \frac{1+\nu}{1-\nu} (\Delta V) b^* \sqrt{3}/(8\pi b^2 Z^2)$ . The distance  $Z$  between the third ( $1\bar{1}1$ ) plane and the glide plane is  $Z = 5b/\sqrt{6}$ . This corresponds to two and a half of the inter-plane distance along the  $[111]$  direction. To provide an estimate of the pinning force we choose  $b^* = b/\sqrt{12}$  which is the edge component of a perfect Shockley partial. The volume variation can be estimated according to a method described in the textbook,<sup>38</sup>  $\Delta V = 3v_{Ni}a_0^{-1}da_0/dC_{Al}$ , where the Vegard's law for Ni(Al) is used to express  $a_0^{-1}da_0/dC_{Al} = 0.0763$ . Then one found  $\alpha = 0.0015$  which is of same order though still larger than what has been found in our simulations (see lines (a3-b3) in Tab.I). If instead of  $b^* = b/\sqrt{12}$ , one chooses the effective Burgers vector computed through a Peierls-Nabarro method<sup>30</sup> then  $\alpha = 0.00083$  which agrees better. A more quantitative study would require the account for the modulus misfit. This comparison allows to emphasize that as a consequence of the edge Burgers components of both partials the size effect dominates the modulus misfit effect often invoked in the analysis of the screw-impurity interaction. Since the partials have some Burgers vectors that are not purely screw, a hydrostatic stress field is localized around the partial cores<sup>39</sup> which renders the partials of a screw similar to the ones of an edge, at the atomic scale. Far away from the center of mass of the dislocation, since the edge components of the leading and the trailing screw partials are opposite, the hydrostatic stress field of both partials annihilate each other and the elastic theory prediction for a purely screw dislocation is recovered. In the first and second ( $1\bar{1}1$ ) planes, the shape of the interaction potential (full and dashed lines in Fig. 3) is imposed by the nonlinear atomic interaction involved during the passage of the impurity through the core of the dislocation. Concerning the pinning strength on a single Al atom, we distinguish a common trend for screw and edge dislocations:<sup>25</sup> The anharmonicity enhances the pinning strength in the compressive regions in regard of the tensile ones. In our simulation cell, the compressive

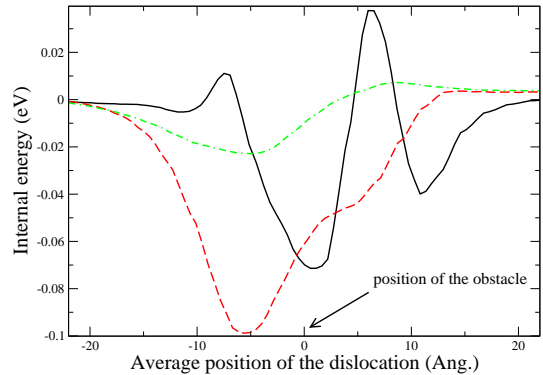


FIG. 3: The internal potential energy for a dissociated screw dislocation against the dislocation obstacle distance. The obstacle is an isolated Al in the ( $1\bar{1}1$ ) planes above the glide plane: the first plane (full line), the second plane (dashed line) and the third one (dot-dashed).

region of the edge dislocation is situated above the glide plane whereas for the screw 2 compressive regions can be distinguished, e.g. below the glide plane for the leading partial and above for the trailing partial. The obstacle labeled a1 (b1) in Tab. I visits the compressive region when it crosses the trailing (leading) partial. In agreement, the stronger pinning strength is found for the trailing (leading) partial. Furthermore the comparison of the pinning strengths in the separated compressive regions shows that the trailing partial is anchored more strongly than the leading one. The same trend can be noted for the tensile regions. Worthily the previous remarks are consistent with the results on the edge dislocation.<sup>25</sup> The latter trend finds some substantiations into the fact that the more stable position of the Al solute is inside the stacking fault ribbon, as can be seen in Fig. 3. The potential energy measured with respect to the isolated Al far away from the dislocation core should yield a diffusion current toward the dislocation stacking fault. This is a Suzuki-type effect which operates on both types of dislocation. This could lead to a classical dynamic strain aging of the fcc substitutional alloys.<sup>40</sup> In our computation the diffusion is frozen and such an effect is thus disregarded as it is indeed in the SSH statistical models discussed below. Another consequence of the absence of the solute diffusion is that there is no short range ordering even for the Al concentrated solid solutions. It must be noticed that the interaction potential with the nearest obstacles (see Fig.3) is far from the simple shape assumed in some more phenomenological approaches<sup>5</sup> and even from an elastic theory<sup>32,41</sup> which neglects the dislocation core geometry. As it is required for the construction of a statistical model, some of the details of the atomic scale must be left off and one must retain only the essential quantities that are identified as important. According to the SSH theory, an obstacle can be characterized by an interaction range  $w$  and a pinning force  $f_m$ , or equivalently a binding energy  $U$ . We thus attempt to

estimate such quantities and to that purpose we chose arbitrarily a rounding method. We distinguish only two different cases depending on the obstacle position with respect to the leading and the trailing partial. For the pinning strength  $\alpha$  we choose the maximum of the interaction force. The definition of the interaction range  $w$  requires a more tactful treatment since in principle the short range obstacle-core interaction is superposed to a long range elastic one and further the interaction potential is not symmetric for an obstacle position ahead and behind the partials, mainly because of the presence of a stacking fault. Around the absolute force maximum, we measure  $w$  as the shortest distance to which the force vanishes or falls to a local minimum. We choose to neglect the variations of the force over that limit. We concede that such a point can be discussed and must be kept in mind for further discussion on the analytical models. We emphasize that we have been primarily concerned with finding a manner to estimate one of the key parameters of the theory,  $w$  and that there is no well prescribed theoretical way for that. We believe that the SSH theory should be developed to address specifically the case of a dissociated dislocation with an interaction potential similar to the one reported in Fig.3 rather than the standard Gaussian-like potentials.

In the present study, when the interaction potential shows a force maximum near the position of one of the partials we ascribe the force to this partial. This is a conventional way of arranging the numerous obstacle forces since the two partials are actually interacting through the stacking fault. Further when the obstacle is attractive for the leading partial and repulsive for the trailing one, the force fields overlap and it may then be difficult to identify with accuracy the interaction range. When it has not been possible to separate different force maximum, we reported the corresponding pinning strength as being exerted on the trailing one (see (b2-b3) lines in Tab.I). In the fcc symmetry, for the Al concentration we are concerned with, the density of the Al dimers has same order as the density of single Al, i.e.  $C_{Al} \approx nC_{Al}^2$  where  $n = 12$  is the number of nearest fcc neighbors. Above  $C_{Al} = 1/n$  the number of isolated Al vanishes in average. It is thus of some interest to study the pinning strength of the Al dimers that might be expected to play a role on the SSH because of the alloy ordering energy. Among the different configurations of pairs, we selected those with a distance between solute atoms corresponding to first, second and some of the third neighbors in the fcc lattice. Either the screw dislocation interacts with preexisting Al dimers referred to as (c-h) in Tab.I or the dislocation passage modifies the Al-Al bond crossing the glide plane (i-p) in Tab.I. For the non-crossing pairs, the (c-e) configurations correspond to the planar dimer situated above the glide plane whereas the (f-h) are below. The directions of the dimer bond before the dislocation passage are  $[011]$  (c) and (f),  $[10\bar{1}]$  (d) and (g),  $[110]$  (e) and (h),  $[011]$ . The dimers that cross the glide plane are oriented in the direction  $[\bar{7}21]$  (i),  $[211]$

TABLE I: Summary of different pinning obstacles for both the leading (subscript  $l$ ) and the trailing partials (subscript  $t$ ) of the screw dislocation, their pinning force  $\alpha$  (normalized by  $\mu b^2$ ) and their force range  $w$ .

| Nature            | text Ref. | $\alpha_l$ and $w_l$  | $\alpha_t$ and $w_t$  |
|-------------------|-----------|-----------------------|-----------------------|
| single            | (a1)      | 0.0020/ 1.14 <i>b</i> | 0.0111/ 0.88 <i>b</i> |
| 1st planes        | (b1)      | 0.0088/ 1.05 <i>b</i> | 0.0059/ 2.20 <i>b</i> |
| single            | (a2)      | 0.0036/ 1.41 <i>b</i> | 0.0032/ 1.69 <i>b</i> |
| 2nd planes        | (b2)      | -                     | 0.0053/ 1.52 <i>b</i> |
| single            | (a3)      | -                     | 0.0011/ 2.8 <i>b</i>  |
| 3rd planes        | (b3)      | -                     | 0.0009/ 2.85 <i>b</i> |
| 1st neighbor      | (c)       | 0.0022/ 0.77 <i>b</i> | 0.0264/ 2.19 <i>b</i> |
| non-crossing pair | (d)       | 0.0006/ 0.1 <i>b</i>  | 0.0139/ 1.49 <i>b</i> |
|                   | (e)       | 0.0033/ 1.03 <i>b</i> | 0.0168/ 1.14 <i>b</i> |
|                   | (f)       | 0.0079/ 0.72 <i>b</i> | 0.0086/ 2.82 <i>b</i> |
|                   | (g)       | 0.0207/ 1.8 <i>b</i>  | 0.0068/ 2.03 <i>b</i> |
|                   | (h)       | 0.0153/ 1.05 <i>b</i> | 0.0106/ 2.33 <i>b</i> |
| 3th neighbor      | (i)       | 0.0094/ 1.24 <i>b</i> | 0.0147/ 2.45 <i>b</i> |
| crossing pair     | (j)       | 0.0026/ 0.43 <i>b</i> | 0.0206/ 2.09 <i>b</i> |
| 2nd neighbor      | (k)       | 0.0137/ 1.24 <i>b</i> | 0.0142/ 2.45 <i>b</i> |
| crossing pair     | (l)       | 0.0184/ 2.87 <i>b</i> | 0.0224/ 2.38 <i>b</i> |
|                   | (m)       | 0.0096/ 1.09 <i>b</i> | 0.0146/ 1.07 <i>b</i> |
| 1st neighbor      | (n)       | -                     | 0.0157/ 1.79 <i>b</i> |
| crossing pair     | (o)       | 0.0171/ 1.87 <i>b</i> | 0.0035/ 1.14 <i>b</i> |
|                   | (p)       | 0.0218/ 2.77 <i>b</i> | 0.0161/ 1.37 <i>b</i> |

(j),  $[212]$  (k),  $[\bar{1}\bar{2}2]$  (l),  $[2\bar{2}\bar{1}]$  (m),  $[4\bar{1}1]$  (n),  $[1\bar{1}4]$  (o) and  $[141]$  (p). Our results on the pinning strength and the interaction range are reported on the corresponding lines in Tab.I. Besides the variable geometry of the crossing pairs, it is worth noting that the pinning strength of a non-crossing dimer does not correspond to the simple superposition of the strength of 2 isolated Al that would be placed at the reticular sites occupied by the dimer. The resulting strength can be even smaller than an isolated Al as seen from the comparison between the single (b1) and the first neighbor dimer (f). It must be also remarked that some of the dimer strengths can be larger than two isolated Al at the same position, e.g. (b1) and (g) in Tab.I. The second neighbor Al dimers could be expected to be more stable than others with regard to the  $L1_2$  ordering trend of the Ni(Al) alloy. Such an expectation is not reflected by the dimer pinning strengths which are not significantly larger to break the second neighbor pairs although the interatomic potential between Ni and Al particles was adjusted to fit the corresponding order energy.<sup>19</sup> The forces reported on lines (k-m) are not particularly stronger than those concerning the first and third neighbor dimers. Finally if one considers the whole set of the dimer configurations, the pinning strengths for a screw dislocation are not smaller than for the edge ones reported in Ref. 25.

### III. ANALYTICAL MODELS FOR COMPUTING THE SOLUTION CRSS

The MS simulations allowed us to perform a direct computation of the CRSS at the atomic scale. In the past, different statistical theories have been proposed to evaluate the CRSS of solid solutions. The common assumption of the various analytical models is that the CRSS can be derived only from a unique interaction of the dislocation with an isolated impurity in the glide plane. Although these statistical models were primarily devoted to the computation of the CRSS for an edge dislocation, there is no theoretical argument against the application of these models to a screw dislocation provided that one is able to quantify the model input parameters. In order to compare consistently the model predictions to our data on the SSH, the model parameters are determined from the average of the single Al pinning configurations (lines (a1) and (b1) in Tab.I). We obtained a single valued obstacle strength  $f_m = \bar{\alpha}\mu b^2$  where  $\bar{\alpha} = 0.007$  is the mean pinning coefficient for the isolated Al situated in the nearest (111) planes. We also computed the typical interaction range as an average over the different isolated obstacle configurations  $\bar{w} = 1.3b$ . Further, since in principle the models apply to an undissociated dislocation, the leading and the trailing partials are assumed to be tightly bound. In the different models, the end formula is usually presented for a theoretical square lattice which leads to an atomic area of  $s = b^2$ . In our system, this is to be changed for  $s = b^2\sqrt{3}/2$ ,<sup>53</sup> i.e. the atomic area in the glide plane.

Another quantity required before going into the details of the models is the dislocation stiffness. In our simulation cell, we computed the dislocation line energy as the difference between the whole atomic potential energy of a simulation cell with a dislocation and the one of a perfect single crystal with same geometry and same atom number. It was then possible to obtain the energy per unit length  $E_L$  of the straight dislocation in pure Ni. One must emphasize that this computation implies the stacking fault energy which is not modeled in the classical estimation of the dislocation energy, i.e.,  $E_L = \mu b^2/2$ . For the edge dislocation, we obtained  $E_{Le} = 0.95E_L$  while for the screw  $E_{Ls} = 0.61E_L$ . These two quantities depend on the simulation cell geometry ( $L_x, L_z$ ) in agreement with the logarithmic law derived from elastic theory. Since in the Ni(Al) solid solution (see Fig.1) the dislocation length depends on the Al distribution, it is not possible to compute the dislocation line energy as done in a pure material where the dislocation is straight. However, one can expect reasonably that  $E_L$  should vary as the elastic shear modulus  $\mu$  and the lattice parameter  $b$ , according to the Vegard's law which leads to a variation of roughly 1 at. % of  $C_{Al}$ . Since such a variation of the dislocation stiffness has not been considered in the SSH theory we shall not account further for such a dependency although for the concentrated solutions it would be worth accounting for it. To obtain the dislocation line tension we apply

a well known result from the isotropic elastic theory<sup>42</sup> which tells us that for the screw  $\Gamma_s = E_{Ls}(1 + \nu)/(1 - \nu)$  while for the edge  $\Gamma_e = E_{Le}(1 - 2\nu)$ . We note that the line tension increase with the cell dimensions will impact the dislocation roughness through the obstacles distribution as it is predicted by some of the following models.

#### A. Fleischer-Friedel theory

One of the classical models to evaluate the strengthening of the solid solution is referred as to the Fleischer-Friedel (FF) model.<sup>37</sup> The model's main assumption is that the dislocation line forms some bows<sup>31</sup> between isolated point-like obstacles randomly distributed. The bow shape assumption contrasts with what can be seen from our simulations in Fig.1. The critical angle associated with the impurity strength is  $\bar{\alpha}_s = f_m/2\Gamma_s$ . The Friedel length is  $L_F = \sqrt{2s\Gamma_s/cf_m}$  where  $c$  is the obstacle concentration which corresponds to  $c = 4C_{Al}$  to account for the different configurations, i.e. above and below the glide plane and for both partials (Tab.I). The CRSS is then given by the balance between the Peach-Koehler force and a meanfield regular array of obstacle  $\tau_c b L_F = f_m$ . The FF end formula reads:

$$\tau_c = \frac{f_m^{3/2} \sqrt{c}}{b\sqrt{2s\Gamma_s}}. \quad (1)$$

The corresponding plot of  $\tau_c$  against the Al density is reported in Fig.2 (a) and (b) for the screw and the edge dislocation, respectively. The FF theory is found to underestimate the CRSS of our simulations. Foreman and Makin<sup>31,43</sup> showed that the Eq.1 overestimates by about 10 % the true CRSS for some perfect point-like obstacle random distribution so that the discrepancy between our simulation and the FF model predictions could not be compensated by such a correction. It is compelling that the FF model is not suitable to compute the CRSS in the concentrated random Ni(Al) solution. One must be reminded however that the FF model proved reliable<sup>31</sup> for some stronger obstacles as precipitates and for smaller densities. It would be interesting to study by MS the lower densities but then the finite size sampling of the Al distribution limits the statistics.

#### B. Mott-Nabarro-Labusch theory

The Mott-Nabarro-Labusch (MNL) theory has been built from different contributions.<sup>3,4,5,15,44,45</sup> The solute dislocation interaction is assumed to be of a finite range  $\bar{w}$  without presuming of the attractive or the repulsive character of the interaction. We introduce the parameter  $v = 2\bar{w}$  which agrees with the definition of Nabarro for the interaction range. The dislocation is still idealized by a perfect elastic string and its configuration is assumed to be a quasi-straight line which interacts with several solute atoms. Alongside the dislocation core, in a ribbon of

length  $2L$  and width  $2v$ , the number of atomic sites in the planes contiguous to the glide plane is  $8vL/s$ . The ribbon extent allows to account for the attractive and repulsive parts of the interaction. Inside this ribbon a counting of the obstacle gives in average  $2n = 8vLc/s$ . The segment is sustained to a mean restoring force which depends on the stiffness of the string. Mott<sup>4</sup> showed that this force could be written as  $2Lf_m^2x/L'v^2\Gamma_s$  where  $x$  is the segment mean position and  $L'$  is the mean distance between two obstacles situated along the segment  $2L$ . The distance  $L'$  is fixed by  $4L'vc/s = 1$ . Nabarro assumed<sup>5</sup> that the characteristic length  $L$  could be identified as the distance above which the string Green's function vanishes:  $L = (L'v\Gamma_s/\sqrt{2}f_m)^{2/3}$ . Following Mott and Nabarro,<sup>3</sup> the counting of the obstacles situated in front and behind the segment  $2L$  leads to a total number of interactions  $2n$  which the average force is  $\pm f_m/2$ . These interactions yield a maximum fluctuation of  $\sqrt{2n}f_m/2$  which must be equated to the external Peach-Koehler force  $2Lb\tau_c$  to obtain the CRSS:

$$\tau_c = \left( \frac{c^2v f_m^4}{b^3s^2\Gamma_s} \right)^{1/3}. \quad (2)$$

Here the obstacles above and below the glide plane have been accounted for. If one assumes that the two partials are bound, one must replace  $c$  with  $2C_{Al}$ . The plot of the corresponding CRSS has been reported in Fig.2 and it is found to underestimate the strengthening for the concentrated solutions. The same results hold for the edge dislocation. It is noteworthy that the MNL model is commonly thought to provide a good description for the high densities. In the case of our Ni(Al) solution, our comparison contrasts with such a belief. However, as for the FF model at smaller densities it is not excluded that the agreement could be recovered. An extended version of the MNL model has been proposed elsewhere<sup>25</sup> to tentatively account for the different types of obstacles, i.e. isolated and clusters with different pinning strength  $f_m$  and interaction range  $w$ . Although this model gave us some satisfactory results for both the edge and the screw dislocation further developments are required to be fully consistent on the theoretical treatment.

### C. Butt-Feltham theory

In the Butt-Feltham (BF) theory,<sup>9,46,47</sup> an undissociated dislocation liberates from a pinning configuration by nucleation of a bulge. This critical bulge can be approximated by a triangle shape of height  $W$  which corresponds to the saddle point energy required to unzip the whole dislocation. According to Feltham  $W$  is estimated from the dislocation core radius extent and thus for a close-packed metals  $W \approx 3b$ . As other previous models in the BF theory it is proposed to relate the CRSS to the in-plane obstacle density. Along the dislocation line the inter-obstacle distance is roughly  $b/\sqrt{c}$ .

For a quantitative comparison we distinguish the mean distance in function of the different geometry for the edge and the screw dislocation:  $\lambda = \sqrt{2}b/\sqrt{c}$  and  $\lambda = b/\sqrt{c}$ , respectively. The enthalpy required to form a bulge is :  $H = UL/\lambda + 2W^2\Gamma/L - \tau bWL/2$  where  $U$  is the binding energy and  $L$  is the bulge extent along the dislocation line. In the expression for  $H$ , one recognizes the binding energy, the elastic cost for the bulge and the work of the Peach-Koehler force. The bulge curvature is determined by the external stress and thus for a certain  $W$  we deduce the corresponding bulge extent  $L = \sqrt{8W\Gamma/\tau b}$ . At the critical configuration, the enthalpy cancels which gives the end result:

$$\tau_c = \frac{4U}{bW\lambda}. \quad (3)$$

We assume that the binding energy can be estimated roughly as  $U = f_m\bar{w}$  and we account for the different obstacle configurations by  $c = 4C_{Al}$ . The corresponding plot has been reported in Figs.2 (a) and 2 (b) for both edge and screw. Although the predicted CRSS is quantitatively of same order as the MS simulation data, the BF theory predicts a  $\tau_c$  in  $\sqrt{C_{Al}}$  which underestimates the hardening rate of our simulations. It should be mentioned that Butt and Feltham also derived different power laws according to the variation of the bulge height  $W$ . With such an extension the BF theory prediction may agree better with the MS data.

### D. Friedel-Mott-Suzuki theory

Another theory proposed by Friedel, Mott and Suzuki (FMS) in their text books<sup>6,8</sup> considers the few atoms around an ideal undissociated dislocation line. This theory allows the dislocation to take locally much larger curvatures than in the FF model. The first effect of this pinning of the dislocation is to give the dislocation a "zigzag" shape. The interaction is characterized by a binding energy  $U$  which we approach by  $f_m\bar{w}$  valid for a linearized force. We briefly recall the model derivation. The amplitude of the zigzag in the glide plane is denoted by  $W$  and its wavelength alongside the dislocation line is denoted by  $L$ . According to Friedel<sup>6</sup> the number of solute contained in the glide plane area  $WL/2$  is given by the inverse of the surface density, i.e.  $WL/2 = s/c$ . However a careful counting leads us to  $WL = s/c$  since the construction of a regular two-dimensional lattice where the obstacles are separated by  $L$  in the  $Y$  direction and  $W$  in the  $X$  direction leads us to  $WL = s/c$  which agrees with Suzuki's derivation.<sup>8</sup> The binding energy per unit of length is  $E_1 = 2f_m\bar{w}/L$ . The line tension energy involved in the zigzag is given by  $E_2 = \Gamma(\sqrt{(W^2 + L^2)/4} - L/2)/(L/2) \approx 2\Gamma W^2/L^2$  at first order in  $W/L$ . By minimizing the difference  $E_2 - E_1$  one obtains the optimal value of the zigzag  $W = (f_m\bar{w}s/4\Gamma c)^{1/3}$  that fixes the line shape and thus  $E_1 = 2\bar{w}Wc/s$  and  $E_2 = 4\Gamma c^2W^4/s^2$ . The application of

external shear stress deforms the dislocation. It has been assumed that the effect of the external shear stress is to unzip the line from the obstacles at the bottom of the zigzag, where the line tension exerts a maximum force in the glide direction. Considering that the maximum of the potential energy is a straight line ( $W = 0$ ), bound to the obstacle situated at the top of the former zigzag, the energy difference between this maximum and the zigzag configuration is  $(-E_1/2) - (E_2 - E_1)$ . Multiplied by the wavelength  $L$  this gives the work that must be provided by the external shear stress to overcome the pinning barrier. The area that is comprised between the two configurations of the line, zigzag and straight is  $WL/2$ , so the stress work is  $\tau_c bWL/2$  which must equal  $(E_1/2 - E_2)L$ . The end result for  $\tau_c$  is:

$$\tau_c = \frac{f_m \bar{w} c}{sb}. \quad (4)$$

Noteworthy this expression for the CRSS does not depend on the line tension in contrast to the other models. To apply the theory to our system, the input parameters are estimated similarly and we assumed that  $c = 4C_{Al}$ . In Fig.2(a) and (b), it is remarkable that the  $\tau_c$  linear dependency in  $C_{Al}$  is much closer from the simulations than a fractional power law. The FMS assumption of a zigzag shape is closer from the wavy profile of the dislocation seen in Fig.1. The agreement between our data and the theory is better for the screw (Fig.2(a)) than for the edge (Fig.2(b)) since for the latter the FMS model slightly overestimates the CRSS. With the force model parameters for a screw dislocation, the amplitude of the zigzag is  $W = 0.43b$  at  $C_{Al} = 2$  at. % and  $W = 0.25b$  at  $C_{Al} = 10$  at. %. Besides the fact that such an amplitude is smaller than what can be depicted in Fig.1, the model predicts  $W$  to decrease with  $C_{Al}$ . We studied the dislocation roughness and found the opposite trend. In view of the discrepancy on the edge CRSS, our procedure to compute the model parameters from our atomistic data can be discussed. To improve this transfer from the atomic scale to a continuous theory, we emphasize that some improvements of the model would be required to account for the dissociation of the dislocation core and the various types of obstacles.

#### IV. SUMMARY AND PERSPECTIVES

The aim of the present paper was to extend the study of CRSS for a solid solution Ni(Al) to a screw dislocation. We carried out two types of computation: (i) the CRSS of a random distribution of solutes at different concentration  $C_{Al}$  and (ii) the pinning strength of some different obstacles, isolated Al or dimers. We found that the CRSS and the pinning strengths of the screw dislocation are of the same order as the edge ones studied elsewhere.<sup>25</sup> Such a result could not be expected from a first order elastic theory which conventionally ascribes the screw pinning to a modulus misfit effect in contrast to the dominant size

effect in the edge case. For the isolated Al impurities, this result has been clearly identified as a consequence of the dissociation of the dislocation core and the edge components of the Shockley partials cores. The Al clusters pinning forces have been shown not to derive from the linear superposition of the isolated obstacle strain field.

Another issue of the present paper was to tentatively apply some analytical models to compute the CRSS. To that purpose, the elementary input parameters of the models were compiled from our atomistic data. The analytical models that we considered only account for the isolated foreign atoms situated in the planes that bound the glide plane. The Friedel-Mott-Suzuki theory provides us a better agreement for the Ni(Al) model solid solution. The estimation of the interaction range between the dislocation and the obstacle is however to be questioned because of the presence of the stacking fault and other nearest obstacles. Our work emphasizes that the SSH theory has to be developed to integrate more of the atomistic details of the dislocation solute interaction. We believe that the accuracy of the SSH theory in the fcc solid solution requires to integrate the dissociation of the dislocation as well as the possibility for cluster formation in the concentrated solution. The farther obstacles as those situated in the second and third (111) planes were found to yield a pinning strength that is not negligible in comparison to the solute atoms that bound the glide plane. We also tested other SSH theories involving mixing laws as the Pythagorean one<sup>48</sup> but they are essentially devoted to model the random distribution of point-like obstacles and finally did not allow us to obtain a better agreement.

To predict quantitatively the CRSS in a variety of materials, we believe that an extended use of the empirical interatomic potentials is not feasible at the present state of our skill in developing such potentials. The recent progress of the first principles calculations for alloys and dislocations<sup>49,50</sup> allows us to expect that the pinning strength could be computed with a better accuracy. However it is difficult to imagine that the statistics could be also studied with such methods because of the associated computational load. The effective interatomic potential can thus be employed to explore the frontier between the atomic details and the SSH statistics as we attempted in the present paper. In the near future, we shall propose to extend our work to the Al(Mg) solid solution. Our motivation rests on the fact that the interatomic potentials were proved physically reliable for the study of the alloy plasticity<sup>20,23</sup> and the physical properties of the Al(Mg) solid solution differ from the Ni(Al) ones, e.g. a larger size effect and a higher stacking fault energy. The temperature effect on the SSH and therefore the dynamics of a dislocation in a disordered media is an eagerly difficult problem at the atomic scale because of the time limit of the molecular dynamics simulations. Moreover some puzzling problems of physics can be anticipated: (i) at the low temperature the inertial effect leads to a loss of strength,<sup>51</sup> (ii) at higher temperature

the activation of the diffusion yields a dynamic aging<sup>23</sup> and (iii) for the intermediate temperature an odd athermal plateau on the yield stress has been clearly identified experimentally for various solutions and remains difficult

to interpret through a simple theory.<sup>5,52</sup> We keep scrutinizing the works about those topics which suffer from a lack of modern investigations.

- 
- <sup>1</sup> R. Cahn, *Nature* **410**, 643 (2001).
- <sup>2</sup> H. Sieurin, J. Zander, and R. Sandstrom, *Mater. Sci. Eng. A* **415**, 66 (2006).
- <sup>3</sup> N. Mott and F. Nabarro, *Report on the Strength of Solids* (Physical Society, London, 1948), pp. 1-19.
- <sup>4</sup> N. Mott, *Imperfections in Nearly Perfect Crystals* (John Wiley, New York, 1952), p.173.
- <sup>5</sup> F. Nabarro, *Dislocations and Properties of Real Materials* (The Institute of Metals, London, 1985), p. 152.
- <sup>6</sup> J. Friedel, *Dislocations* (Addison-Wesley, New York, 1964), p. 224.
- <sup>7</sup> P. Haasen, *Dislocations in Solids*, vol. 4 (North-Holland, Amsterdam, 1979), p. 155.
- <sup>8</sup> T. Suzuki, S. Takeuchi, and H. Yoshinaga, *Dislocation Dynamics and Plasticity* (Springer-Verlag, Berlin Heidelberg, 1991), p. 32.
- <sup>9</sup> M. Butt and P. Feltham, *Phys. Stat. Sol. A* **60**, 167 (1980).
- <sup>10</sup> D. Chandrasekaran, *Mater. Sci. Eng. A* **309**, 184 (2001).
- <sup>11</sup> Y. M. Blanter and V. Vinokur, *Phys. Rev. B* **66**, 2002 (2002).
- <sup>12</sup> S. Brazovskii and T. Nattermann, *Adv. Phys.* **53**, 177 (2004).
- <sup>13</sup> P. Chauve, T. Giamarchi, and P. L. Doussal, *Phys. Rev. B* **62**, 6241 (2000).
- <sup>14</sup> A. Rosso, P. L. Doussal, and K. Wiese, *Phys. Rev. B* **75**, 220201 (2007).
- <sup>15</sup> R. Labusch, *Phys. Status Solidi* **41**, 659 (1970).
- <sup>16</sup> D. Rodney and G. Martin, *Phys. Rev. B* **61**, 8714 (2000).
- <sup>17</sup> R. Picu and D. Zhang, *Acta Mater.* **52**, 161 (2004).
- <sup>18</sup> K. Tapasa, D. Bacon, and Y. N. Osetsky, *Mater. Sci. and Eng. A* **400**, 109 (2005).
- <sup>19</sup> E. Rodary, D. Rodney, L. Proville, Y. Bréchet, and G. Martin, *Phys. Rev. B* **70**, 054111 (2004).
- <sup>20</sup> D. Olmsted, L. Hector, W. Curtin, and R. Clifton, *Model. Simul. Mater. Sci. Eng.* **13**, 371 (2005).
- <sup>21</sup> E. Bitzek and P. Gumbsch, *Mater. Sci. Eng. A* **400**, 40 (2005).
- <sup>22</sup> J. Marian and A. Caro, *Phys. Rev. B* **74**, 24113 (2006).
- <sup>23</sup> W. Curtin, D. Olmsted, and L. Hector, *Nature Materials* **5**, 875 (2006).
- <sup>24</sup> K. Tapasa, D. Bacon, and Y. N. Osetsky, *Model. Simul. Mater. Sci. Eng.* **14**, 1153 (2006).
- <sup>25</sup> L. Proville, D. Rodney, Y. Bréchet, and G. Martin, *Phil. Mag.* **86**, 3893 (2006).
- <sup>26</sup> D. Tabor, *The Hardness of Metals* (Oxford University Press, 1951).
- <sup>27</sup> M. Y. Gutkin, I. Ovid'ko, and C. Pande, *Phil. Mag.* **84**, 847 (2004).
- <sup>28</sup> J. Hirth and J. Lothe, *Theory of dislocations* (Wiley Interscience, New York, 1982), p. 510.
- <sup>29</sup> B. Joos and M. S. Duesbery, *Phys. Rev. Lett.* **78**, 266 (1997).
- <sup>30</sup> M. P. P. Szelestey and K. Kaski, *Model. Simul. Mater. Sci. Eng.* **11**, 883 (2003).
- <sup>31</sup> A. Foreman and M. Makin, *Phil. Mag.* **14**, 911 (1966).
- <sup>32</sup> R. A. S. Patu and D. Esterling, *Metallurgical Transactions A* **20**, 1411 (1989).
- <sup>33</sup> J. Angelo, N. Moody, and M. Baskes, *Modell. Simul. Mater. Sci. Eng.* **3**, 289 (1995).
- <sup>34</sup> A. Voter and S. Chen, *Mater. Res. Soc. Symp. Proc.* **82**, 175 (1987).
- <sup>35</sup> M. Baskes, X. Sha, J. Angelo, and N. Moody, *Modelling Simul. Mater. Sci. Eng.* **5**, 651 (1997).
- <sup>36</sup> H. Saka, *Dislocations in Solids* (University of Tokyo Press, 1985), p. 251.
- <sup>37</sup> R. Fleischer and W. Hibbard, *Proc. Conf. at N.P.L.* **1**, 262 (1963).
- <sup>38</sup> J. Friedel, *Dislocations* (Addison-Wesley, New York, 1964), p. 362.
- <sup>39</sup> M. Wen, A. Ngan, S. Fukuyama, and K. Yokogawa, *Phil. Mag.* **85**, 1917 (2005).
- <sup>40</sup> M. C. Chen, L. Chen, and T. Lui, *Acta metall. mater.* **40**, 2433 (1992).
- <sup>41</sup> G. Gremaud and S. Kustov, *Phys. Rev. B* **60**, 9353 (1999).
- <sup>42</sup> J. Hirth and J. Lothe, *Theory of dislocations* (Wiley Interscience, New York, 1982), p. 176.
- <sup>43</sup> T. Nogaret and D. Rodney, *Phys. Rev. B* **74**, 134110 (2006).
- <sup>44</sup> F. Nabarro, *Phil. Mag.* **35**, 613 (1977).
- <sup>45</sup> R. Labusch, *Acta Metall.* **20**, 917 (1972).
- <sup>46</sup> M. Butt, I. Ghauri, R. Qamar, K. Hashmi, and P. Feltham, *Act. Metall.* **29**, 829 (1981).
- <sup>47</sup> M. Butt, *Jour. of Mat. Sci* **28**, 2557 (1993).
- <sup>48</sup> M. Hiratani and V. Bulatov, *Phil. Mag. Lett.* **84**, 461 (2004).
- <sup>49</sup> N. I. Medvedeva, Y. N. Gornostyrev, and A. J. Freeman, *Phys. Rev. B* **76**, 212104 (2007).
- <sup>50</sup> L. Ventelon and F. Willaime, *J. Computer-Aided Mater. Des.* **14**, 85 (2008).
- <sup>51</sup> R. Isaac and A. Granato, *Phys. Rev. B* **37**, 9278 (1988).
- <sup>52</sup> H. Suzuki, *International Conference Dislocations and Mechanical Properties of Crystals* (J. Wiley and Sons, 1957), p. 361.
- <sup>53</sup> This corrects a mistake on  $s$  introduced in Ref.<sup>25</sup> with no consequence on the end results in same reference